Ion-induced mixing and demixing in the immiscible Ni-Ag system

Thomas J. Colla and Herbert M. Urbassek
Fachbereich Physik, Universität Kaiserslautern, Erwin-Schrödinger-Straße, D-67663 Kaiserslautern, Germany

Kai Nordlund and Robert S. Averback
Materials Research Laboratory, University of Illinois, Urbana, Illinois 61801

(Received 7 July 2000; revised manuscript received 30 October 2000; published 20 February 2001)

By molecular-dynamics simulation, we study the effect of 10 keV primary knock-on atoms (PKA's) on a Ni-Ag interface, and a homogeneous random $Ni_{0.5}Ag_{0.5}$ alloy. The interface roughens; compact islands of 1 ML thickness are created. Only a few isolated impurity atoms are formed. Effects in the random alloy are stronger. It decomposes, creating Ag- and Ni-rich regions. Due to the different lattice constants of the elements, both the interface and in particular the random alloy amorphize. The thermal spike created by the PKA persists longer in the random alloy, due to heating by the large positive heat of mixing of the Ni-Ag system. Comparison with simulation of Cu-Ag demonstrates that the demixing in Ni-Ag derives from its immiscibility in the liquid phase.

DOI: 10.1103/PhysRevB.63.104206 PACS number(s): 61.82.Bg, 79.20.Rf, 81.40.Wx

I. INTRODUCTION

Ion bombardment of binary compounds induces atomic relocation and hence chemical mixing in these systems.[1] Most investigations of this phenomenon have concentrated on ion-induced effects in miscible systems and ordered alloys.[2–5] Ion-bombardment effects, however, are also of interest in immiscible systems. In addition to the possibility of creating metastable materials, these systems are interesting from a fundamental point of view, since the mixing effect of ion bombardment is counteracted by the decomposing effect of chemistry, which tends to segregate the species.[6–9] Up to now, molecular-dynamics studies on ion-induced mixing in segregating systems have been rare.[10,11]

In the present investigation, we concentrate on the Ni-Ag system, which has a high positive heat of mixing, such that its equilibrium phase diagram not only exhibits immiscibility in the solid state, but even a miscibility gap in the liquid.[12] We study the effects induced by a 10 keV primary knock-on atom (PKA). Cu-Ag is also investigated since it provides a particularly illuminating system for comparison. First, Cu and Ag are immiscible in the solid state but not the liquid state. The atomic sizes of Cu and Ni, moreover, are very similar in relationship to the much larger Ag atom, and thus possible size effects on mixing are avoided in this comparison. The simulations, therefore, can elucidate the relative roles of ballistic, liquid-state diffusion, and solid-state diffusion in the mixing process. We study two extreme geometries: (i) a sharp interface between Ni and Ag that becomes mixed by the ion bombardment and (ii) random stoichiometric alloys $Ni_{0.5}Ag_{0.5}$ and $Cu_{0.5}Ag_{0.5}$. While it is difficult to prepare the $Ni_{0.5}Ag_{0.5}$ system experimentally, we shall consider it here primarily as a model system, which presents an extreme case to emphasize decomposition effects. The focus of the present work is thus to elucidate the kinetics of mixing in energetic displacement cascades, and in particular, to determine in which phases of the cascade evolution the mixing/demixing actually takes place.

II. SYSTEM

For Ni-Ag we employ a many-body potential,[13] which has been designed to incorporate the main features of the elemental systems; we note, in particular, that Ni has a smaller lattice constant, and a higher cohesive energy, bulk modulus, and melting temperature, than Ag. The positive heat of mixing between Ag and Ni, which is 238 meV/atom for the $Ni_{0.5}Ag_{0.5}$ alloy according to Miedema's theory,[14,15] is also incorporated into our potential. The potential cutoff radius is $r_c = 6.0$ Å for both elements. Our computation cell contains 248 270 atoms for the interface system and 269 500 atoms in the alloy system; it is enclosed in energy-dissipating boundaries. We simulate for 20 ps. For Cu-Ag we used the original Foiles EAM potential.[16] This system is immiscible in the solid state, but the heat of mixing is very close to zero (0.02 eV/atom according to Miedema's theory, 0.04 eV/atom in our model). All the potentials used were smoothly joined to the Ziegler-Biersack-Littmark interatomic potential[17] to realistically describe high-energy collisions. The simulation and analysis procedures for Cu-Ag were the same as for the Ni-Ag alloy.

Due to the importance of the melting temperature for our system, we determined the melting temperatures of elemental Ni and Ag for our potential. Here we used a method analogous to that described in Ref. 18, in which a liquid-solid interface is established, and the temperature is sought where the interface is in stable equilibrium; of course, the simulation volume needs to be adapted such that the pressure stays zero. We found 1255 K for Ag which compares well with the experimental value of 1235 K; for Ni our value of 1550 K is 10% smaller than the experimental value (1728 K). This deviation does not affect the qualitative results of this study, as the substantial difference in melting temperatures is preserved.

In the Cu-Ag system, Ag has experimentally about a 100 K lower melting point than Cu. We checked that this also holds for the Foiles model,[16] obtaining melting points of 1150 K for Ag and 1280 K for Cu.

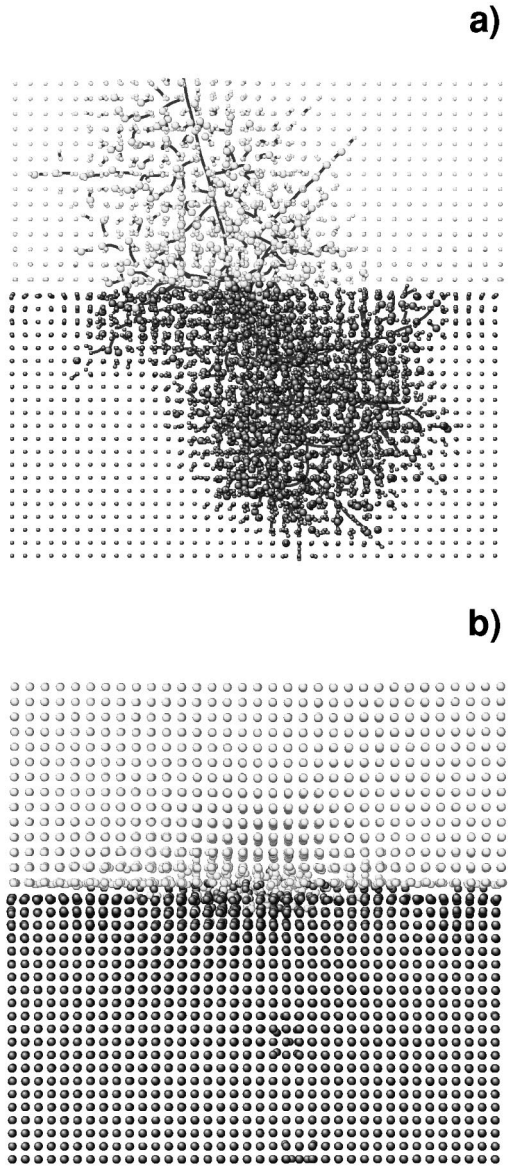

FIG. 1. Cross-sectional view through the Ni-Ag interface system at 0.15 ps (a) and 20 ps (b) after the start of a 10 keV Ag PKA at 30 Å from the interface. Light: Ag. Dark: Ni. Small dots: atoms that have not yet moved.

III. INTERFACE

We construct a (100) $\Sigma 1$ interface and let it relax while we cool the system to 0 K. We note that this $\Sigma 1$ interface does not have the lowest energy among all (100) interfaces,[19] but we chose it here for convenience. A 10 keV Ag PKA starts at a distance of 30 Å from the interface and is directed towards it in a non-channeling direction.

Figure 1 shows the interface at 150 fs, i.e., while still in the linear-collision-cascade regime, and also at 20 ps, after the cascade motion has ended. A complete animation is available.[20] Here, only the central zone (containing 26 564 atoms) is shown. The figure shows that while the collision cascade covers a large volume on both sides of the interface, the final disorder is restricted to the immediate vicinity of the interface and this region has become partly amorphized. This

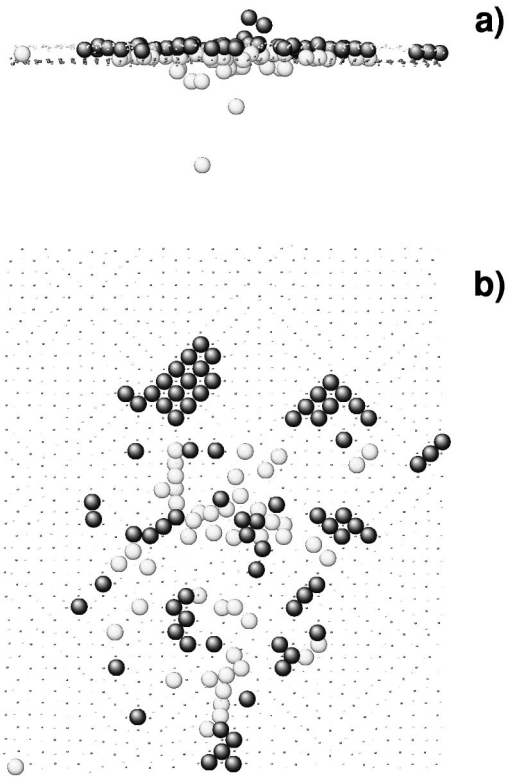

FIG. 2. Side (a) and top (b) view on the interface at 20 ps after the start of a 10 keV Ag PKA. Only those atoms are shown that have moved beyond the interface, i.e., the plane positioned in the middle between the Ni and Ag half spaces. Light: Ag. Dark: Ni. Small dots: nonrelocated interface atoms.

is most likely a consequence of the difference in lattice constants of Ni and Ag. Only a few atoms have been displaced far into the other side of the interface. Figure 2 provides side and top views of the interface itself. Only those atoms are shown that have moved beyond the interface, i.e., the plane positioned midway between the Ni and Ag half spaces. It is seen that these relocated atoms cluster mostly at the layer immediately bounding the initial interface, forming islands and thus reducing the chemical contribution to the interface energy.

Figure 3 plots against time the number of *intruder* atoms, which we define as all those atoms that have moved at least 0.5 monolayers across the interface. Their number is remarkably small. Only 4 Ni and 14 Ag atoms are thus effectively mixed in this system. We attribute the strong asymmetry observed between Ni and Ag intruders to the higher binding energy of Ni atoms, which makes them more resistant to displacement. This feature can be quantified by the higher activation energy for diffusion that was also observed in a previous model study of thermal effects in the Ni-Ag system.[13] Asymmetric mixing behavior has also been observed in Cu/Ni and Cu/Co.[11] Furthermore, as Fig. 2 showed, some Ag atoms—but no Ni atoms—were recoil implanted deeply into the other side of the interface; this happens simply because the cascade was started from the Ag-side of the interface.

Figure 4 offers some details of the central energized zone

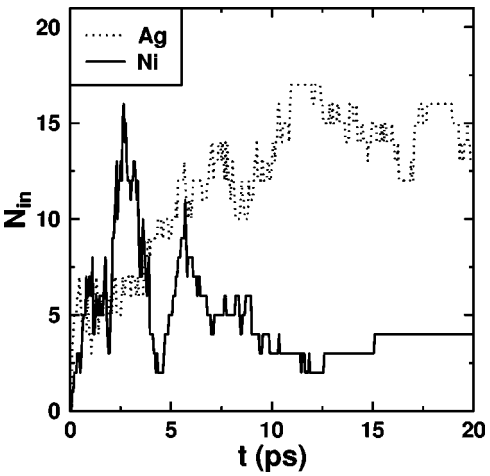

FIG. 3. Time evolution of the number of intruder atoms, defined as all those atoms which have been relocated at least 0.5 ML to the other side of the interface.

of the collision cascade. We concentrate on the number of *molten* atoms, defined as those atoms that have a kinetic energy above $3kT_m/2$, where T_m is the melting temperature of Ni. The molten zone exists until roughly 5 ps, showing that a rather long-lived thermal spike has been created. The number of molten Ni atoms is larger than the number of molten Ag atoms despite its higher melting temperature; this, however, is a direct consequence of the collision cascade being situated more on the Ni side of the interface. Note that the thermal histories of the Ag and the Ni subsystems are well correlated, proving that both subsystems are in good energetic contact during this spike phase. Figure 4(b) displays the temporal evolution of the density in the molten zone; the density is calculated as the average of the density in spheres around each molten atom with radius equal to the potential cutoff radius r_c. The reduced density, which is typical of thermal spikes,[21,22] is clearly observed.

We also followed three additional Ag PKA's and four Ni PKA's, varying systematically the start distance to the interface. The results were all qualitatively similar to those described above. We observed no systematic dependence of the results on the point of initiation other than the obvious fact that interface mixing was maximized when the interface lay in the center of the collision cascade. We note, however, that interface mixing—as quantified by the number of intruders—was systematically smaller for Ni PKA's than for Ag PKA's. We attribute this to the fact that Ni stopping in Ni is considerably smaller than Ag stopping in Ag;[23] hence the deposited energy density and thus the temperature of the spike formed will be higher for Ag than for Ni PKA's.

IV. ALLOY

We construct a $Ni_{0.5}Ag_{0.5}$ crystal by placing Ni and Ag atoms randomly on an fcc lattice. The lattice constant is taken from Vegard's law, i.e., as the arithmetic mean of the elemental lattice constants. The system is then allowed to relax to 0 K. In Fig. 5 we display a cut through the smallest cuboid (containing 9,700 atoms) that completely contains the

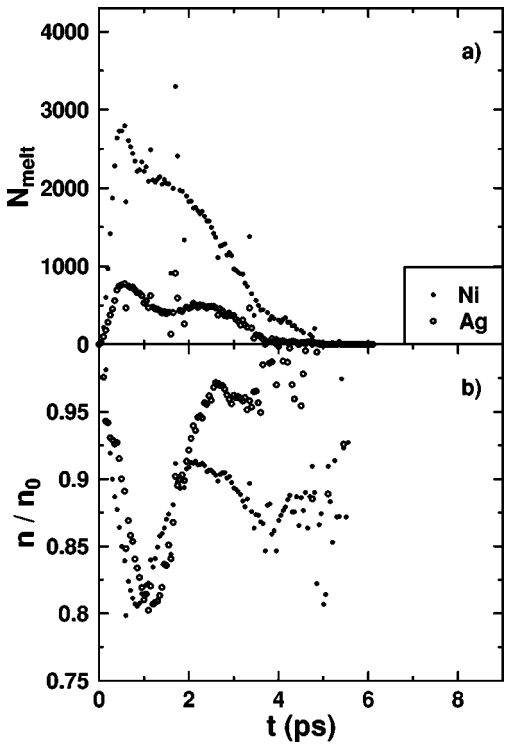

FIG. 4. Number of molten atoms (a) and density (b) in the molten zone of the spike initiated by the 10 keV Ag PKA in the Ni-Ag interface system. The density is normalized to the solid density n_0 of elemental Ni and Ag, respectively. All atoms are considered molten that have a kinetic energy above $3kT_m/2$, where $T_m = 1728$ K is the melting temperature of Ni.

molten zone of the bombarded crystal. Figure 5(a) shows the alloy before ion irradiation, and Fig. 5(b) shows a cross section through the alloy at 20 ps after the start of a 10 keV Ag PKA. A complete animation for this event is also available.[20] The changes observed are considerably stronger than in the interface system. Most notably, the alloy has undergone decomposition, forming Ag- and Ni-rich regions. Due to the high number of minority (solute) atoms in these enriched regions—which is far above the equilibrium solubility limit—and due to the incompatibility of the elemental lattice constants, these regions did not crystallize after the thermal spike, and they appear amorphous. Note that the initial state of our system—the random alloy—is in fact thermodynamically strongly unstable; thus the energy delivered by the PKA can be considered to trigger the spinodal decomposition of this alloy.

Figure 6 shows the number of molten atoms and the density reduction in the spike region, in close analogy to Fig. 4 for the interface system. While the trends are similar, we can observe that the spike in the alloy persists for a longer time than in the interface system. This is due, in part, to the large positive heat of mixing, which is delivered to the system during the decomposition process. This energy refuels the spike as it evolves. A difference in the heat conductivity of the random alloy, as compared to that of the interface system, may also be relevant, although these conductivities were not determined.

In order to understand the different clustering behavior of

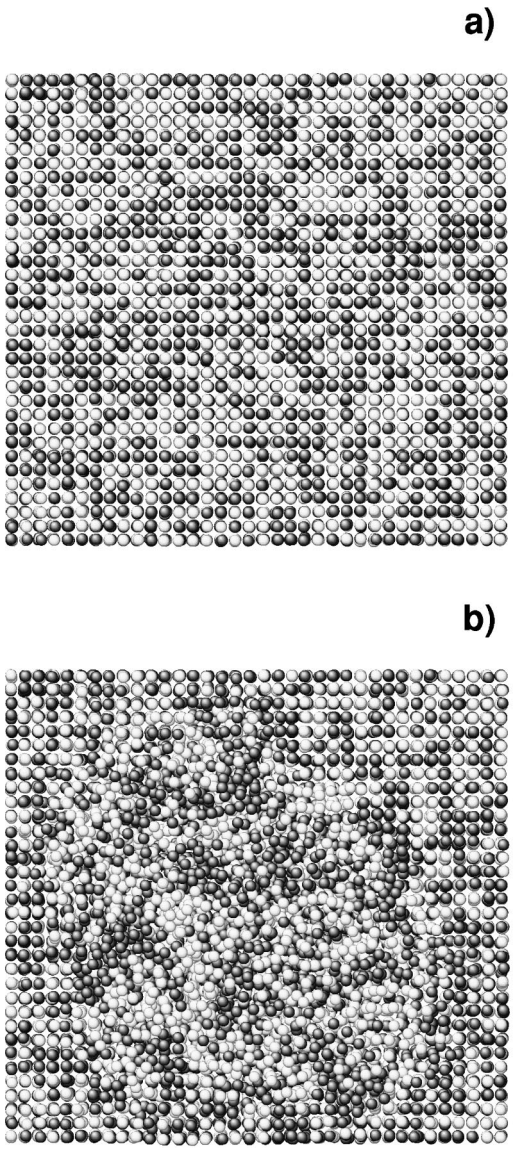

FIG. 5. Cross-sectional view through the $Ni_{0.5}Ag_{0.5}$ alloy system before (a) and 20 ps (b) after the start of a 10 keV Ag PKA. Light: Ag. Dark: Ni.

Ag and Ni atoms, we plot in Fig. 7 the probabilities $P_{ij}(z)$ that an i atom has exactly z j neighbors. We count all those atoms as nearest neighbors to a given atom that are closer to it than the arithmetic mean of the first- and the second-neighbor distances in the ideal Vegard's-law lattice. These data are based on the ensemble of molten atoms, as presented in Fig. 6. While prior to irradiation [Fig. 7(a)], at $t=0$, the $P_{ij}(z)$ curves all coincide and are symmetrically shaped around the maximum at $z=6$, the data presented in Fig. 7(b) show three typical features which evolved in the system after ion irradiation.

(1) The number of Ag-Ni bonds is dramatically reduced; the pertinent distribution P_{AgNi} exhibits now a maximum at $z=4$.

(2) The P_{NiNi} distribution has broadened and now extends to $z=14$.

(3) The P_{AgAg} distribution has remained rather sharp, but its maximum has increased to $z=7$.

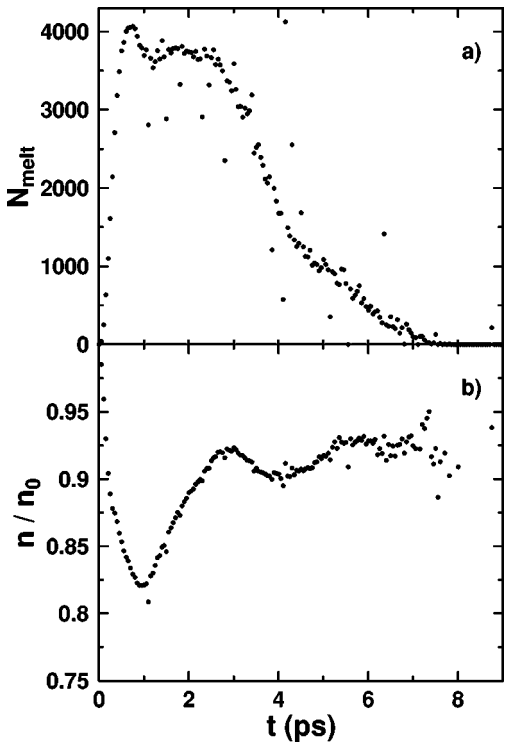

FIG. 6. Number of molten atoms (a) and density (b) in the molten zone of the spike initiated by a 10 keV Ag PKA in the $Ni_{0.5}Ag_{0.5}$ alloy system. The density is normalized to the average density n_0 of elemental Ni and Ag. All atoms are considered molten that have a kinetic energy above $3kT_m/2$, where $T_m=1728$ K is the melting temperature of Ni.

These observations quantify the clustering behavior due to ion irradiation. Items 2 and 3 show that clustering proceeds differently for Ag and Ni atoms. One reason is the different sizes of Ag and Ni atoms, which has the consequence that our procedure for identifying nearest neighbors allows more nearest neighbors around Ni atoms (in the amorphous structure) than it does around Ag ones. Furthermore, the different clustering may also be influenced by the lower melting temperature of Ag, which allows more segregation in the Ag-rich regions than in the Ni-rich ones.

In order to quantify the time evolution of the decomposition process, we calculate the short-range-order parameter γ_i, which we define for each species i (Ni or Ag) separately. Denoting by Z_i the number of nearest neighbors around an i atom, and by z_i the number of its nearest neighbors of the same species, then[13]

$$\gamma_i=\left\langle \frac{z_i-0.5Z_i}{0.5Z_i} \right\rangle. \tag{1}$$

Here, the brackets denote the average over all i-atoms in the molten zone. Initially, at time $t=0$, due to the construction of our system as a random fcc crystal, each atom has $Z_i=12$ nearest neighbors, of which on the average $z_i=6$ belong to the same species; hence, $\gamma_i=0$. γ_i is connected to the average $\langle z_i \rangle$ that can be obtained from the probabilities

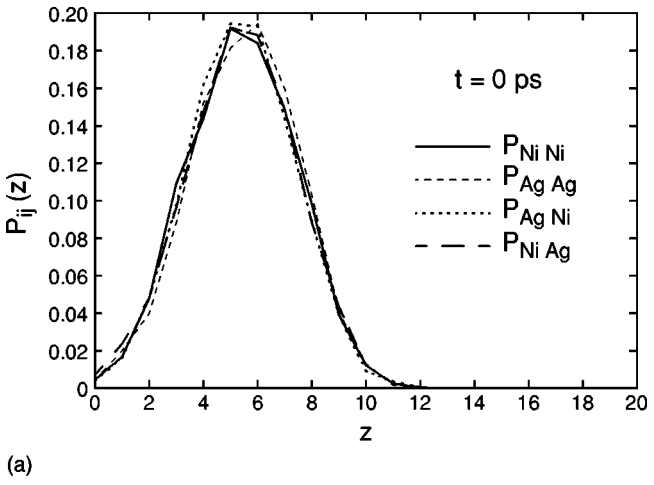

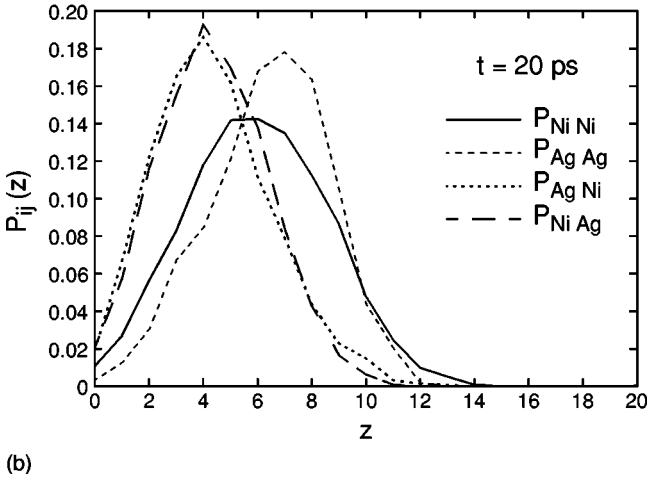

FIG. 7. Probabilities $P_{ij}(z)$ that an i atom has exactly z j neighbors in its first-neighbor shell in the $Ni_{0.5}Ag_{0.5}$ alloy. Data have been evaluated in the ensemble of all atoms that have at some time been molten, see Fig. 6. Data taken (a) before irradiation ($t=0$), (b) after irradiation ($t=20$ ps).

$P_{ij}(z)$ of Fig. 7, but in a nontrivial way, since the total number of nearest neighbors Z_i will change from atom to atom.

Figure 8 gives us the time scale of decomposition. In order to quantify it, we fit our simulation data to a function of the form

$$\gamma(t)=\gamma_{\text{final}}\text{erf}\sqrt{\alpha t}. \tag{2}$$

We chose this functional form after experimenting with several other forms.[13] While γ_{final} gives the limiting value of the short-range-order parameter acquired at large times, α measures the time rate of decomposition. The maximum value of the short-range-order parameter γ_{final} is considerably larger for Ag than for Ni. Indeed, when inspecting Fig. 5(b), one may obtain the impression that Ag atoms tend to form the larger clusters, which are surrounded by Ni atoms. This corresponds to the data shown in Fig. 7 and discussed above. Note that the absolute numbers of γ_{final} depend on the size of the molten zone for which mixing was evaluated (here 5544 atoms) and hence need not be discussed. The decomposition rates α_i obtained from the fit were $1.2(1.4)\times10^{11}$ /s for Ni

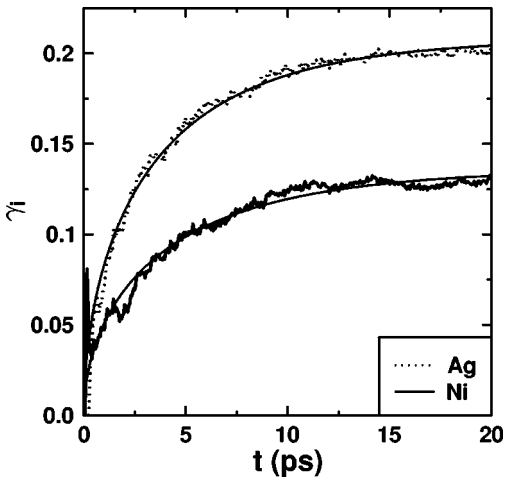

FIG. 8. Time evolution of the short-range-order parameter γ_i of Ag and Ni atoms. Dashed: Fit according to Eq. (2).

(Ag), which are the same to within the uncertainty of the fits. These high rates highlight the speed with which decomposition proceeds. We assume that the major part of decomposition takes place in the hot, low-density liquid phase—note

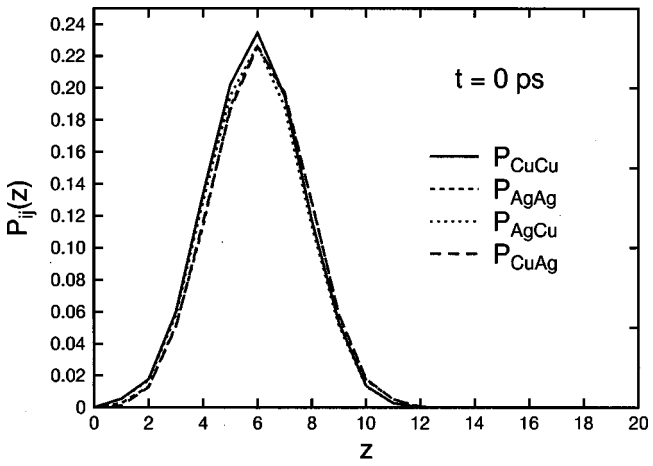

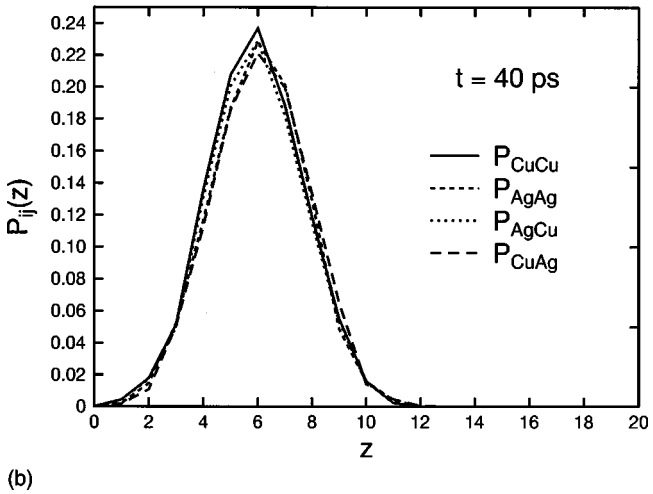

FIG. 9. As in Fig. 7, but for $Cu_{0.5}Ag_{0.5}$.

that the positive heat of mixing of this system is so large that the system exhibits a miscibility gap even in the liquid part of the equilibrium phase diagram; this fact is reproduced by our potential.[13] It is noteworthy that these relaxation times are about a factor of 2 larger than the relaxation time for atoms to fall below their melting points, as seen in Fig. 6(a). This suggests that segregation continues in the supercooled liquids and presumably most abundantly in the Ag-rich regions. In a previous study,[13] we determined decomposition rates of random Ni-Ag alloys as a function of temperature and density in a homogeneous model system. The high rates encountered in the present simulation match those of the model study[13] at temperatures around or slightly above 3000 K.

We also studied the changes in the short-range order of the alloy induced by 1 keV PKA's. Here we used an ensemble of 40 PKA's—each starting in a freshly constructed, relaxed fcc random alloy. The average size of the molten zone comprised 240 atoms. The average value of γ_{final} in the molten zone was 0.01 for Ni and 0.08 for Ag. Hence it appears that even in these small-scale spikes, a certain amount of demixing is possible. Again we attribute the asymmetry primarily to the lower binding energy (melting temperature) of Ag, and also to the change in the number of nearest neighbors around the differently sized atoms.

Turning to Cu-Ag, we plot P_{ij} for this system in Figs. 9(a) and 9(b). Here it is observed that the distributions remain virtually unchanged by the cascades, clearly illustrating the lack of segregation effects in this system. Since more atomic diffusion within cascades is expected in the Cu-Ag system than in the Ni-Ag system,[24] we can conclude that the lack of demixing in Cu-Ag is a consequence of its liquid miscibility and not a consequence of the kinetics. One of the effects of Cu-Ag remaining a homogeneous alloy is that it reforms a crystal after the melt zone has resolidified. In Ni-Ag, which does undergo phase separation on a very fine scale, the quenched-in structure becomes amorphous. Apparently the large size misfit between the Ni and Ag is too large to form coherent phase boundaries and the large density of incoherent phase boundaries between Ni-rich and Ag-rich grains raises the free energy of the two-phase systems above that of the amorphous phase. This observation is consistent with the work of Wolf *et al.*, Ref. 25, which showed that when the grain sizes of even elemental solids becomes too small, the system transforms to an amorphous phase. The comparison of mixing in Ni-Ag and Cu-Ag also suggests that all of the atomic motion occurs while the atoms in the hot zone are in the liquid state. Otherwise, segregation would have been observed in Cu-Ag as well as Ni-Ag. Finally we note that segregation effects are indeed possible within the brief lifetime of the thermal spike. While it has long been realized that mixing can occur during the thermal spike, the present study demonstrates that the kinetics of disordering reactions are sufficiently fast to be important in displacement cascades.

V. CONCLUSIONS

In conclusion, we showed that ion bombardment of the immiscible Ni-Ag system induces both mixing and decomposition. An initially sharp Ni-Ag interface becomes mixed due to the ion bombardment; however, only few atoms are relocated so far to the other side of the interface as to become isolated impurities. Rather, the interface is roughened on a 1 ML scale. A PKA in a random $Ni_{0.5}Ag_{0.5}$ alloy, on the other side, induces a strong decomposition of the system, forming Ni- and Ag-rich zones. Due to the large mismatch in the lattice constants in the Ni-rich and Ag-rich phases, the system amorphizes in the center of the thermal spike formed. The smaller, shorter-lived and cooler spikes induced by 1 keV PKA's lead to less demixing, which is furthermore restricted almost exclusively to the (lower-melting) Ag subsystem. Demixing and amorphization in a similarly prepared Cu-Ag alloy was not observed, illustrating that demixing in displacement cascades requires that the alloy components be immiscible in the liquid phase and that solid-state immiscibility is not sufficient for phase separation.

ACKNOWLEDGMENTS

T.J.C. acknowledges support by the Deutsche Forschungsgemeinschaft and K.N. financial support from the Academy of Finland and grants of computer time from the Center for Scientific Computing in Espoo, Finland. The work at UIUC was supported by the U. S. Department of Energy BES under Grant No. DEFG-96ER45439.

[1] R.S. Averback and T. Diaz de la Rubia, in *Solid State Physics*, edited by H. Ehrenreich and F. Spaepen (Academic Press, Boston, 1998), Vol. 51, p. 281.

[2] T. Diaz de la Rubia, A. Caro, and M. Spaczer, Phys. Rev. B **47**, 11 483 (1993).

[3] M. Spaczer, A. Caro, M. Victoria, and T. Diaz de la Rubia, Phys. Rev. B **50**, 13 204 (1994).

[4] D.J. Bacon and T. Diaz de la Rubia, J. Nucl. Mater. **216**, 275 (1994).

[5] H. Zhu, R.S. Averback, and M. Nastasi, Philos. Mag. A **71**, 735 (1995).

[6] J. Fine, T.D. Andreadis, and F. Davarya, Nucl. Instrum. Methods Phys. Res. **209/210**, 521 (1983).

[7] D. Marton, J. Fine, and G.P. Chambers, Phys. Rev. Lett. **61**, 2697 (1988).

[8] Z.J. Zhang, O. Lin, and B.X. Liu, Phys. Rev. B **51**, 8076 (1995).

[9] A. Crespo-Sosa, P. Schaaf, W. Bolse, K.-P. Lieb, M. Gimbel, U. Geyer, and C. Tosello, Phys. Rev. B **53**, 14 795 (1996).

[10] H. Gades and H.M. Urbassek, Phys. Rev. B **51**, 14 559 (1995).

[11] K. Nordlund and R.S. Averback, Phys. Rev. B **59**, 20 (1999).

[12] R. Hultgren, *Selected Values of the Thermodynamic Properties of Binary Alloys* (American Society for Metals, Metals Park, Ohio, 1973).

[13] T.J. Colla, H.M. Urbassek, and R.S. Averback, Nucl. Instrum.

Methods Phys. Res. B **153**, 369 (1999).
[14] F.R. de Boer *et al.*, in *Cohesion in Metals: Transition Metal Alloys* (North-Holland, Amsterdam, 1989), p. 298.
[15] A.R. Miedema, Philips Tech. Rev. **36**, 217 (1976).
[16] S.M. Foiles, M.I. Baskes, and M.S. Daw, Phys. Rev. B **33**, 7983 (1986).
[17] J. F. Ziegler, J. P. Biersack, and U. Littmark, in *Stopping Powers and Ranges of Ions in Matter*, edited by J. F. Ziegler (Pergamon, New York, 1985), Vol. 1.
[18] J.R. Morris, C.Z. Wang, K.M. Ho, and C.T. Chan, Phys. Rev. B **49**, 3109 (1994).
[19] Y. Gao, S.A. Dregia, and P.G. Shewmon, Acta Metall. **37**, 1627 (1989).
[20] T.J. Colla and H.M. Urbassek, http://www.physik.uni-kl.de/urbassek, 1998.
[21] A.J.E. Foreman, W.J. Phythian, and C.A. English, Philos. Mag. A **66**, 671 (1992).
[22] T.J. Colla and H.M. Urbassek, Radiat. Eff. Defects Solids **142**, 439 (1997).
[23] P. Sigmund, in *Sputtering by Particle Bombardment I*, edited by R. Behrisch (Springer, Berlin, 1981), p. 9.
[24] S.-J. Kim, M.-A. Nicolet, R.S. Averback, and D. Peak, Phys. Rev. B **37**, 38 (1988).
[25] P. Keblinski, D. Wolf, S.R. Phillpot, and H. Gleiter, Philos. Mag. Lett. **76**, 143 (1997).